

# LT-OCF: Learnable-Time ODE-based Collaborative Filtering

Jeongwhan Choi, Jinsung Jeon, Noseong Park

{jeongwhan.choi,jjsjjs0902,noseong}@yonsei.ac.kr

Yonsei University

Seoul, South Korea

## ABSTRACT

Collaborative filtering (CF) is a long-standing problem of recommender systems. Many novel methods have been proposed, ranging from classical matrix factorization to recent graph convolutional network-based approaches. After recent fierce debates, researchers started to focus on *linear* graph convolutional networks (GCNs) with a *layer combination*, which show state-of-the-art accuracy in many datasets. In this work, we extend them based on neural ordinary differential equations (NODEs), because the linear GCN concept can be interpreted as a differential equation, and present the method of Learnable-Time ODE-based Collaborative Filtering (LT-OCF). The main novelty in our method is that after redesigning linear GCNs on top of the NODE regime, i) we learn the optimal architecture rather than relying on manually designed ones, ii) we learn smooth ODE solutions that are considered suitable for CF, and iii) we test with various ODE solvers that internally build a diverse set of neural network connections. We also present a novel training method specialized to our method. In our experiments with three benchmark datasets, Gowalla, Yelp2018, and Amazon-Book, our method consistently shows better accuracy than existing methods, e.g., a recall of 0.0411 by LightGCN vs. 0.0442 by LT-OCF and an NDCG of 0.0315 by LightGCN vs. 0.0341 by LT-OCF in Amazon-Book. One more important discovery in our experiments that is worth mentioning is that our best accuracy was achieved by dense connections rather than linear connections.

## KEYWORDS

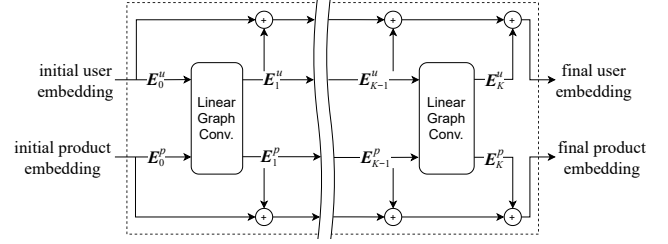
Collaborative Filtering, Neural Ordinary Differential Equation

### ACM Reference Format:

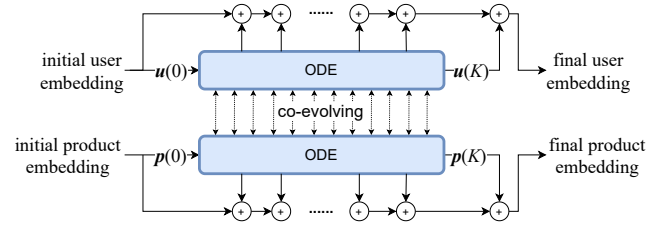
Jeongwhan Choi, Jinsung Jeon, Noseong Park. 2021. LT-OCF: Learnable-Time ODE-based Collaborative Filtering. In *CIKM '21: ACM International Conference on Information and Knowledge Management*, November 01–05, 2021, Queensland, Australia. ACM, New York, NY, USA, 12 pages. <https://doi.org/10.1145/nnnnnnnn.nnnnnnnn>

## 1 INTRODUCTION

Collaborative filtering (CF), which is to predict users' preferences from patterns, is a long-standing research problem in the field of recommender systems [1, 6, 11, 18, 21, 22, 32, 37, 41, 43]. It is common to learn user and product embedding vectors and calculate their dot-products for recommendation. Matrix factorization is one such approach, which is well-known in the recommender system community [22]. There have been proposed several other enhancements as well [17, 20]. Recently researchers started to focus on graph convolutional networks (GCNs) for the purpose of CF [5, 16, 34]. GCNs had been proposed to process not only CF-related graphs



(a) The architecture of LightGCN. The outer loop created by a series of additions, denoted  $\oplus$ , is called *layer combination*.



(b) Our proposed LT-OCF. The detailed diagram of the ODE layer is in Fig. 5.

**Figure 1: (a) The linear architecture of LightGCN with a layer combination, and (b) Our proposed LT-OCF. In our design, two ODEs for user and product embeddings co-evolve over time and influence each other.**

but also other general graphs. GCNs are broadly categorized into the following two types: spectral GCNs [3, 8, 19, 36, 38] and spatial GCNs [2, 13–15, 31]. GCNs for CF fall into the first category due to its appropriateness for CF [4, 16].

However, there have been fierce debates about what is the optimal GCN architecture for CF. During its early phase, researchers utilized non-linear activations, such as ReLU, because they showed good accuracy in many machine learning tasks, e.g., classification, regression, and so on [30, 33–35, 42]. Surprisingly, however, it was recently reported that a *linear* GCN architecture with a *layer combination*, called LightGCN, works better than other non-linear GCNs for CF [5, 16, 34]. Unlike other general graphs, user-product interaction bipartite graphs are frequently sparse and provide little information because they mostly do not include node/edge features. In [16], it was noted that, for the same reason, non-linear GCNs are quickly overfitted to training data and do not work well in general for CF.

Owing to the discovery, we propose the method of Learnable-Time ODE-based Collaborative Filtering (LT-OCF) in this paper. We redesign the linear GCN with the layer combination on top of the

concept of the neural ordinary differential equations (NODEs) because linear GCNs, including LightGCN, can be theoretically interpreted as differential equations, i.e., heat equations (see Section 2.4). For instance, the main linear propagation layer of LightGCN is exactly the same as Newton’s law of cooling.

Neural ordinary differential equations (NODEs) are to learn implicit differential equations from data. NODEs calculate  $\mathbf{h}(t_1) = \mathbf{h}(t_0) + \int_{t_0}^{t_1} f(\mathbf{h}(t), t; \theta_f) dt$ , where  $f$  is a neural network parameterized by  $\theta_f$  that approximates  $\frac{d\mathbf{h}(t)}{dt}$ , to derive  $\mathbf{h}(t_1)$  from  $\mathbf{h}(t_0)$ , where  $t_1 > t_0$ . We note that  $\theta_f$  is trained from data — in other words,  $\frac{d\mathbf{h}(t)}{dt}$  is trained from data. The variable  $t$  is called as *time variable*, which represents the layer concept of neural networks. Note that  $t$  is a non-negative integer in conventional neural networks whereas it can be any arbitrary non-negative real number in NODEs. In this regard, NODEs are considered as *continuous* generalizations of neural networks.

Various ODE solvers can solve the integral problem, and it was also known that they can generalize various neural network architectures [7]. For instance, the general form of the residual connection can be written as  $\mathbf{h}(t+1) = \mathbf{h}(t) + f(\mathbf{h}(t); \theta)$ , which is identical to the explicit Euler method to solve ODE problems. It is also known that the fourth-order Runge–Kutta (RK4) ODE solver is similar to dense convolutional networks and fractal neural networks [25].

The reason of our specific design choice to adopt NODEs for CF is threefold. In our proposed LT-OCF, firstly,  $t$  is not only *continuous* but also *trainable* because we interpret linear GCNs as continuous-time differential equations. Therefore, we can learn the optimal layer combination construction rather than relying on a manually configured one. Let  $\mathbf{E}_i^u \in \mathbb{R}^{N \times D}$  and  $\mathbf{E}_i^p \in \mathbb{R}^{M \times D}$ , where  $N$  is the number of users,  $M$  is the number of products, and  $D$  is the dimensionality of embedding space, be the user and product embeddings at layer  $i$ , respectively. In recent GCN-based CF methods [5, 16], for instance, the final user embeddings are calculated, owing to the *layer combination* technique, by  $w_0 \mathbf{E}_0^u + w_1 \mathbf{E}_1^u + w_2 \mathbf{E}_2^u + \dots + w_K \mathbf{E}_K^u$ , where  $w_i$  is a coefficient and  $K$  is the number of layers. On the other hand, one contribution of LT-OCF is to calculate  $w_0 \mathbf{u}(0) + w_1 \mathbf{u}(t_1) + w_2 \mathbf{u}(t_2) + \dots + w_K \mathbf{u}(t_K)$ , where  $\mathbf{u}(k)$  corresponds to  $\mathbf{E}_k^u$ ,  $t_i$  is trainable for all  $i$ , and  $t_i < t_j$  if  $i < j$ .

Secondly, NODEs learn homeomorphic functions which we consider suitable for CF — see our discussion after Proposition 2.1. In the recent linear GCN architecture of CF [16], in addition, user/product embedding is simply a weighted sum of neighbors’ embeddings, which can be solely written as matrix multiplications. We also use only matrix multiplications for defining our ODE formulation and matrix multiplication is an analytic operator. The Cauchy–Kowalevski theorem states, in such a case, that the optimal solution of  $\mathbf{h}(t)$  always exists and is unique [12]. Therefore, our ODE-based CF is a well-posed problem (see Section 3.3.1).

After formulating CF as an ODE problem, thirdly, we test with various ODE solvers that internally create a rich set of neural network connections. For instance, residual connections are the same as the explicit Euler method, dense connections are the same as RK4, and so on. We can test with various connections.

The architecture of LT-OCF is shown in Fig. 1 (b). To enable the proposed concept, we define dual co-evolving ODEs, whose detailed diagram is in Fig. 5. There exists an ODE for each of the

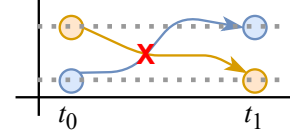


**Figure 2: The locations of the yellow and blue points are inverted by the mapping from  $t_0$  to  $t_1$ . NODEs are not able to learn the yellow and blue trajectories at the same time, which cross each other, because their topology (i.e., their relative positions) cannot be changed after a mapping in NODEs, i.e., homeomorphic mapping.**

user and product embeddings. However, they influence each other and co-evolve over time in our architecture. We also propose a novel training method to train LT-OCF because we have to train dual co-evolving ODEs with their time points  $\{t_1, t_2, \dots\}$ .

We use three CF datasets, Gowalla, Yelp2018, and Amazon-Book, and compare LT-OCF with state-of-the-art methods, such as NGCF [34], LightGCN [16], and so forth, to name a few. Our method consistently outperforms all those methods in all cases. The biggest enhancement is made for Amazon-Book, i.e., a recall of 0.0411 by LightGCN vs. 0.0442 by LT-OCF and an NDCG of 0.0315 by LightGCN vs. 0.0341 by LT-OCF. We also show that i) our method can be trained faster than LightGCN and ii) dense connections are better than linear connections for CF. To our knowledge, we are the first who reports that dense connections outperform linear connections in CF. Our contributions can be summarized as follows:

- (1) We revisit state-of-the-art linear GCNs and propose the method of Learnable-Time ODE-based Collaborative Filtering (LT-OCF) based on NODEs.
- (2) In LT-OCF, we learn the optimal layer combination rather than relying on manually designed architectures.
- (3) We reveal that dense connections are better than linear connections for CF (see Section 5). To our knowledge, we first report this observation.
- (4) We show that our formulation is theoretically well-posed, i.e., its solution always exists and is unique (see Section 3.3).
- (5) LT-OCF consistently outperforms all existing methods in three benchmark datasets.

## 2 PRELIMINARIES & RELATED WORK

We introduce our literature survey and preliminary knowledge to understand our work.

### 2.1 Neural Ordinary Differential Equations (NODEs)

NODEs solve the following integral problem to calculate  $\mathbf{h}(t_{i+1})$  from  $\mathbf{h}(t_i)$  [7]:

$$\mathbf{h}(t_{i+1}) = \mathbf{h}(t_i) + \int_{t_i}^{t_{i+1}} f(\mathbf{h}(t), t; \theta_f) dt, \quad (1)$$

where  $f(\mathbf{h}(t), t; \theta_f)$ , which we call *ODE function*, is a neural network to approximate  $\dot{\mathbf{h}} \stackrel{\text{def}}{=} \frac{d\mathbf{h}(t)}{dt}$ . To solve the integral problem,

NODEs rely on ODE solvers, e.g., the explicit Euler method, the Dormand–Prince (DOPRI) method, and so forth [9].

Let  $\phi_t : \mathbb{R}^{\dim(\mathbf{h}(t_0))} \rightarrow \mathbb{R}^{\dim(\mathbf{h}(t_1))}$  be a mapping from  $t_0$  to  $t_1$  created by an ODE after solving the integral problem. It is well-known that  $\phi_t$  becomes a homeomorphic mapping:  $\phi_t$  is continuous and bijective and  $\phi_t^{-1}$  is also continuous for all  $t \in [0, T]$ , where  $T$  is the last time point of the time domain [10, 26]. From this characteristic, the following proposition can be derived:

**PROPOSITION 2.1.** *The topology of the input space of  $\phi_t$  is preserved in its output space, and therefore, trajectories crossing each other cannot be represented by NODEs, e.g., Fig. 2.*

While preserving the topology, NODEs can perform machine learning tasks and it was shown in [39] that it increases the robustness of representation learning to adversarial attacks and unexpected inputs. We consider that this characteristic is also suitable for learning reliable user/product representations, i.e., embeddings, when there is no abundant information. As mentioned earlier, CF typically includes only user-product interactions without additional user/product features. LightGCN [16] showed that, in such a case, linear GCNs with zero non-linearity, which are known to be *smooth* [4], are appropriate. We conjecture that NODEs that learn smooth (homeomorphic) functions are also suitable for CF for the same reason.

Instead of the backpropagation method, the adjoint sensitivity method is used to train NODEs for its efficiency and theoretical correctness [7]. After letting  $\mathbf{a}_{\mathbf{h}}(t) = \frac{dL}{d\mathbf{h}(t)}$  for a task-specific loss  $L$ , it calculates the gradient of loss w.r.t model parameters with another reverse-mode integral as follows:

$$\nabla_{\theta_f} L = \frac{dL}{d\theta_f} = - \int_{t_m}^{t_0} \mathbf{a}_{\mathbf{h}}(t)^\top \frac{\partial f(\mathbf{h}(t), t; \theta_f)}{\partial \theta_f} dt.$$

We modify the above standard adjoint sensitivity method to design our training algorithm. In our framework, we learn both user/product embeddings and time points  $\{t_1, t_2, \dots\}$  to construct a layer combination using the modified method.

It is known that NODEs have a couple of advantages. First, NODEs can sometimes significantly reduce the required number of parameters when building neural networks [27]. Second, NODEs enable us to interpret the time variable  $t$  as continuous, which is discrete in conventional neural networks [7]. We fully enjoy the second advantage while designing our method.

Fig. 3 shows the typical architecture of NODEs which we took from [10] – we assume a downstream classification task in this figure. There is a feature extraction layer which provides  $\mathbf{h}(0)$ , and  $\mathbf{h}(1)$  is calculated by the method described above. After that, there is a classification layer. In our case, however, we use the architecture in Fig. 1 (b), which has dual co-evolving ODEs only, because our task is not classification but CF.

## 2.2 Residual/Dense Connections and ODE Solvers

Many researchers discuss about the analogy between residual/dense connections and ODE solvers. ODE solvers discretize time variable  $t$  and convert an integral into many steps of additions. For instance,

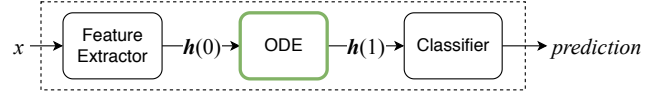


Figure 3: The typical architecture of NODEs

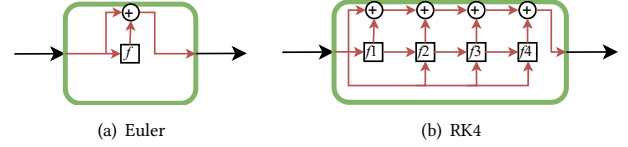


Figure 4: The explicit Euler method and RK4 in a step. To derive  $\mathbf{h}(t+s)$  from  $\mathbf{h}(t)$  with a step size  $s$ , RK4 is four times more complicated than the explicit Euler method. Note that the explicit Euler method is the same as the residual connection and RK4 is the same as the dense connection when  $f$  is a neural network layer.

the explicit Euler method can be written as follows in a step:

$$\mathbf{h}(t+s) = \mathbf{h}(t) + s \cdot f(\mathbf{h}(t), t; \theta_f), \quad (2)$$

where  $s$ , which is usually smaller than 1, is a configured step size of the Euler method. Note that this equation is identical to a residual connection when  $s = 1$ .

Other ODE solvers use more complicated methods to update  $\mathbf{h}(t+s)$  from  $\mathbf{h}(t)$ . For instance, the fourth-order Runge–Kutta (RK4) method uses the following method:

$$\mathbf{h}(t+s) = \mathbf{h}(t) + \frac{s}{6} (f_1 + 2f_2 + 2f_3 + f_4), \quad (3)$$

where  $f_1 = f(\mathbf{h}(t), t; \theta_f)$ ,  $f_2 = f(\mathbf{h}(t) + \frac{s}{2}f_1, t + \frac{s}{2}; \theta_f)$ ,  $f_3 = f(\mathbf{h}(t) + \frac{s}{2}f_2, t + \frac{s}{2}; \theta_f)$ , and  $f_4 = f(\mathbf{h}(t) + sf_3, t + s; \theta_f)$ .

It is also known that dense convolutional networks (DenseNets [44]) and fractal neural networks (FractalNet [23]) are similar to RK4 (as so are residual networks to the explicit Euler method) [25]. For simplicity but without loss of generality, however, we use the explicit Euler method as our running example.

One more ODE solver that is worth mentioning is the implicit Adams–Moulto method which is written as follows:

$$\mathbf{h}(t+s) = \mathbf{h}(t) + \frac{s}{24} (9f_1 + 19f_2 - 5f_3 + f_4), \quad (4)$$

where  $f_1 = f(\mathbf{h}(t+s), t+s; \theta_f)$ ,  $f_2 = f(\mathbf{h}(t), t; \theta_f)$ ,  $f_3 = f(\mathbf{h}(t-s), t-s; \theta_f)$ , and  $f_4 = f(\mathbf{h}(t-2s), t-2s; \theta_f)$ . Both  $f_3$  and  $f_4$  are from previous history and we do not need to newly evaluate them.

This implicit method is different from the aforementioned explicit solvers in that i) it uses past multi-step history, i.e.,  $f_3$  and  $f_4$ , to calculate a more robust derivative term and ii) it uses  $f_1$  in conjunction with the multi-step history. At the moment of time  $t$ , however, it is before calculating  $\mathbf{h}(t+s)$  so evaluating  $f_1$  cannot be done in a naive way. It uses advanced methods, such as Newton’s method, to solve for  $\mathbf{h}(t+s)$ . The use of  $f_1$  is called *implicit* in the field of numerical methods to solve ODEs. Its analogy to neural network connection has not been studied yet due to the implicit nature of the method. However, it falls into the category of dense networks because it uses multi-step information.

For our experiments, we consider all those advanced solvers, which is one more advantage of our formulating the graph-based CF as the dual co-evolving ODEs.

### 2.3 Collaborative Filtering (CF)

Let  $E_0^u \in \mathbb{R}^{N \times D}$  and  $E_0^p \in \mathbb{R}^{M \times D}$  be the initial user and product embeddings, respectively. There are  $N$  users and  $M$  products, and embeddings are  $D$  dimensions. Early CF methods include matrix factorization [22], SVD++ [20], neural attentive item similarity [17], and so on. All these methods utilize user-product interaction history [43].

Because user-product relationships can be represented by bipartite graphs, it recently became popular to adopt GCNs for CF [5, 16, 34]. NGCF is one of the most popular GCN-based CF methods. It uses non-linear activations and transformation matrices to transform from the user embedding space to the product embedding space, and vice versa. At each layer, user and product embeddings are extracted as in the layer combination. However, it concatenates them instead of taking their sum. Its overall architecture is similar to the standard GCN [19]. However, it was later noted that the adoption of the non-linear activation and the embedding space transformation are not necessary in CF due to the environmental dissimilarity between general graph-based downstream tasks and CF [16]. That is, other graph-based tasks include abundant information, e.g., high-dimensional node features. However, CF frequently includes a bipartite graph without additional features. Even worse, the graph is sparse in CF. Due to the difference, non-linear GCNs are easily overfitted to training graphs and their testing accuracy is mediocre in many cases even with various countermeasures preventing it. It was also empirically proven that transforming between user and product embedding spaces is not helpful in CF [16].

After NGCF, several methods have been proposed. Among them, in particular, one recent graph-based method, called LightGCN, shows state-of-the-art accuracy in many datasets. In addition, it also showed that linear GCNs with layer combination work the best among many design choices. Its linear graph convolutional layer definition is as follows:

$$\begin{aligned} E_k^u &= \tilde{A}_{u \rightarrow p} E_{k-1}^p, \\ E_k^p &= \tilde{A}_{p \rightarrow u} E_{k-1}^u, \end{aligned} \quad (5)$$

where  $\tilde{A}_{p \rightarrow u} \in [0, 1]^{M \times N}$  is a normalized adjacency matrix of the graph from products to users and  $\tilde{A}_{u \rightarrow p} \in [0, 1]^{N \times M}$  is also defined in the same way but from users to products. LightGCN learns the initial embeddings, denoted  $E_0^u$  and  $E_0^p$ , and uses the layer combination, which can be written as follows:

$$\begin{aligned} E_{final}^u &= \sum_{i=0}^K w_i E_i^u, \\ E_{final}^p &= \sum_{i=0}^K w_i E_i^p, \end{aligned} \quad (6)$$

where  $K$  is the number of layers,  $w_i$  is a coefficient, and  $E_{final}^u$  and  $E_{final}^p$  are the final embeddings.

The CF methods, including our method, LightGCN, and so on, learn the initial embeddings of users and products (and model

parameters if any). After a series of  $K$  graph convolutional layers, a graph-based CF algorithm derives  $E_{final}^u$  and  $E_{final}^p$  and use their dot products to predict  $r_{u,i}$ , a rating (or ranking score) by user  $u$  to product  $i$ , for all  $u, i$ . Ones typically use the following Bayesian personalized ranking (BPR) loss [29] to train the initial embedding vectors (and model parameters if any) in the field of CF:

$$L = - \sum_{u=1}^N \sum_{i \in \mathcal{N}_u} \sum_{j \notin \mathcal{N}_u} \ln \sigma(r_{u,i} - r_{u,j}) + \lambda \|E_0^u \odot E_0^p\|^2, \quad (7)$$

where  $\mathcal{N}_u$  is a set of products neighboring to  $u$ ,  $\sigma$  is a non-linear activation, and  $\odot$  means the concatenation operator. We use the softplus for  $\sigma$ .

### 2.4 Linear GCNs and Newton's Law of Cooling

As a matter of fact, Eq. (5) is similar to the heat equation, which describes the law of thermal diffusive processes, i.e., Newton's Law of Cooling. The heat equation can be written as follows:

$$\frac{dH_t}{dt} = -\Delta H_t, \quad (8)$$

where  $\Delta$  is the Laplace operator and  $H_t$  is a column vector which contains the temperatures of the nodes in a graph or a discrete grid at time  $t$ . The Laplace operator  $\Delta$  is simply a matrix multiplication with the Laplacian matrix or the normalized adjacency matrix.

Therefore, the right-hand side of Eq. (5) can be reduced to Eq. (8) if we interpret each element of  $E_i^u$  and  $E_i^p$  as a temperature value — since they are  $D$ -dimensional vectors, we can consider that  $D$  different diffusive processes exist in Eq. (5). In this regard, we can consider that LightGCN models discrete thermal diffusive processes whereas our method describes continuous thermal diffusive processes.

## 3 PROPOSED METHOD

In this section, we describe our proposed method. Our main idea is to design co-evolutionary ODEs of user and product embeddings with a continuous and learnable time variable  $t$ .

### 3.1 Overall Architecture

In Fig. 1 (b), we show the overall architecture of LT-OCF. The two initial embeddings,  $E_0^u$  and  $E_0^p$ , are fed into the dual co-evolutionary ODEs. Then, we have the layer combination architecture to derive the final embeddings. The distinguished feature of LT-OCF lies in the dual ODE layer, where we can interpret the time variable  $t$  as a continuous layer variable.

LT-OCF enjoys the continuous characteristic of  $t$  and construct a more flexible architecture. In LightGCN and other existing GCN-based CF methods, we have to use pre-determined discrete architectures. However, LT-OCF can use any positive real numbers for  $t$  and those numbers are even trainable in our case.

### 3.2 ODE-based User and Product Embeddings

The user and product embedding co-evolutionary processes can be written as follows:

$$\begin{aligned} \mathbf{u}(K) &= \mathbf{u}(0) + \int_0^K f(\mathbf{p}(t))dt, \\ \mathbf{p}(K) &= \mathbf{p}(0) + \int_0^K g(\mathbf{u}(t))dt, \end{aligned} \quad (9)$$

where  $\mathbf{u}(t) \in \mathbb{R}^{N \times D}$  is a user embedding matrix and  $\mathbf{p}(t) \in \mathbb{R}^{M \times D}$  is a product embedding matrix at time  $t$ .  $f(\mathbf{p}(t))$  outputs  $\frac{d\mathbf{u}(t)}{dt}$  and  $g(\mathbf{u}(t))$  outputs  $\frac{d\mathbf{p}(t)}{dt}$ .  $\mathbf{u}(0) = E_0^u$  and  $\mathbf{p}(0) = E_0^p$  in our case because the initial embeddings are directly fed into the ODEs (cf. Fig. 1 (b)). We note that  $\mathbf{u}(t)$  and  $\mathbf{p}(t)$  constitute a set of co-evolving ODEs. User embedding influences product embedding and vice versa. Therefore, our co-evolving ODEs are a reasonable design choice.

However, this formulation does not fully describe our proposed concept of *learnable-time* and we propose a more advanced formulation in the next paragraph.

**3.2.1 Learnable-time Architecture.** In our framework, we can learn how to construct the layer combination (rather than relying on a manually designed architecture). In order to adopt such an advanced option, we extract  $\mathbf{u}(t)$  and  $\mathbf{p}(t)$  with several different learnable time-points  $t \in \{t_1, \dots, t_T\}$ , where  $T$  is a hyperparameter, and  $0 < t_i < t_{i+1} < K$  for all  $i$ . Therefore, Eq. (9) can be re-written as follows:

$$\begin{aligned} \mathbf{u}(t_1) &= \mathbf{u}(0) + \int_0^{t_1} f(\mathbf{p}(t))dt, \\ \mathbf{p}(t_1) &= \mathbf{p}(0) + \int_0^{t_1} g(\mathbf{u}(t))dt, \\ &\vdots \\ \mathbf{u}(K) &= \mathbf{u}(t_T) + \int_{t_T}^K f(\mathbf{p}(t))dt, \\ \mathbf{p}(K) &= \mathbf{p}(t_T) + \int_{t_T}^K g(\mathbf{u}(t))dt, \end{aligned} \quad (10)$$

where  $t_i$  is trainable for all  $i$ . The parts of the equation highlighted in red are used to create residual connections (cf. the red residual connections inside the ODEs in Fig. 5). The final embeddings are calculated as follows:

$$\begin{aligned} E_{final}^u &= w_0 \mathbf{u}(0) + \sum_{i=1}^T w_i \mathbf{u}(t_i) + w_K \mathbf{u}(K), \\ E_{final}^p &= w_0 \mathbf{p}(0) + \sum_{i=1}^T w_i \mathbf{p}(t_i) + w_K \mathbf{p}(K). \end{aligned} \quad (11)$$

Recall that what the explicit Euler method does internally is to generalize residual connections in a continuous manner. So, extracting intermediate ODE states (i.e.,  $\mathbf{u}(t)$  and  $\mathbf{p}(t)$  with  $t \in \{t_1, \dots, t_T\}$ ) and creating a higher level of layer combination in Eq. (11) correspond to dual residual connections (cf. the blue layer combination outside the ODEs in Fig. 5).

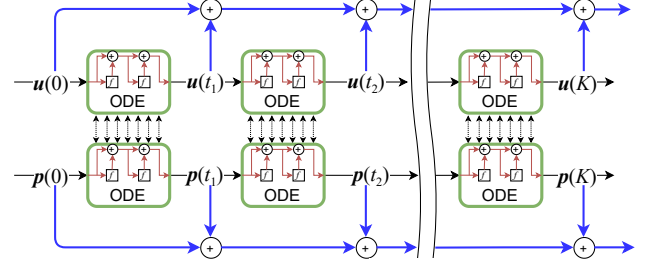


**Figure 5: Our proposed dual co-evolving ODEs.** In this figure, we assume the explicit Euler method. The residual connections inside the ODEs are in red and the layer combination is in blue. The time-points  $\{t_1, \dots, t_T\}$  to construct the layer combination are trained in our framework. In this figure, each ODE internally uses two steps (i.e., two red residual connections) to solve an integral problem but this is only for illustration purposes. In real environments, the number of steps for each ODE can be varied.

**Table 1: Various network architectures (inside and outside the ODEs in Fig. 5) created by various ODE solvers**

ODE Solver	Inside the ODEs	Outside the ODEs
Explicit Euler (without the red parts in Eq. (10))	Linear Connection	Layer Combination
Explicit Euler (with the red parts in Eq. (10))	Residual Connection	
RK4	DenseNet or FractalNet	
Adams-Moulto	Implicit Connection	
DOPRI	Adaptive Connection	

If using other advanced ODE solvers, the connections inside the ODEs become more sophisticated, e.g., DenseNet or FractalNet connections if RK4 is used. In Table 1, we summarize all those cases.

**3.2.2 Non-parameterized and Non-time-dependent ODEs.** We need to define the two ODE functions,  $f$  and  $g$ . Being inspired by the recent success of linear graph convolutions, we use the following definition for  $f$  and  $g$ :

$$\begin{aligned} f(\mathbf{p}(t)) &= \bar{\mathbf{A}}_{u \rightarrow p} \mathbf{p}(t), \\ g(\mathbf{u}(t)) &= \bar{\mathbf{A}}_{p \rightarrow u} \mathbf{u}(t), \end{aligned} \quad (12)$$

where  $\bar{\mathbf{A}}$  means either the symmetric normalized Laplacian matrix or the normalized adjacency matrix. LightGCN uses the latter but our method based on the continuous thermal diffusive differential equation can use both of them.

We note that our definitions for  $f$  and  $g$  will result in non-parameterized and non-time-dependent ODEs because our ODE functions do not require  $t$ ,  $\theta_f$ , and  $\theta_g$  as their input.

**3.2.3 Relation with Linear GCN-based CF Methods.** There exist several linear GCNs. LightGCN studied about the similarity among



various such linear GCN models and showed many other linear models can be approximated as a special case of LightGCN. In this subsection, we study about the similarity between our method and LightGCN.

Suppose the following setting in our method: i)  $t_i$  is not trained but fixed to  $i$  for all  $i$ , ii) We use the explicit Euler method with its step size parameter  $s = 1$ , and iii) We do not use the residual connection but the linear connection inside the ODEs, i.e., removing the red parts in Eq. (10). This specific setting can be written as follows:

$$\begin{aligned} \mathbf{u}(1) &= f(\mathbf{p}(0)), \\ \mathbf{p}(1) &= g(\mathbf{u}(0)), \\ &\vdots \\ \mathbf{u}(K) &= f(\mathbf{p}(K-1)), \\ \mathbf{p}(K) &= g(\mathbf{u}(K-1)). \end{aligned} \quad (13)$$

After that, the linear combination yields  $E_{final}^u = \sum_{i=0}^K w_i \mathbf{u}(t_i)$  and  $E_{final}^p = \sum_{i=0}^K w_i \mathbf{p}(t_i)$ . We note that these final embeddings are equivalent to Eq. (6) because our ODE functions  $f$  and  $g$  in Eq. (12) are equivalent to the linear layer definition of LightGCN in Eq. (5). Thus, our method is equivalent to LightGCN under the specific setting. Therefore, one can consider our method, LT-OCF, as a *continuous* generalization of linear GCNs, including LightGCN and others that can be approximated by LightGCN.

### 3.3 How to Train.

Our proposed method includes a couple of sophisticated techniques and its training algorithm is inevitably more complicated than other cases. We also use the BPR loss, denoted  $L$ , to train our model, which is common for many CF methods.

We propose to alternately train the co-evolving ODEs and their intermediate time points. When training for one, we fix all other parts. This makes the gradient calculation by the adjoint sensitivity method simple because a fixed ODE/time point can be considered as constants at a moment of training time. The gradients of loss w.r.t.  $\mathbf{u}(0)$ , which is identical to the initial embedding  $E_0^u$ , can be calculated via the following reverse-mode integration [7]:

$$\frac{dL}{d\mathbf{u}(0)} = \mathbf{a}_u(K) - \int_K^0 \mathbf{a}_u(t)^\top \frac{\partial g(\mathbf{u}(t))}{\partial \mathbf{u}(t)}, \quad (14)$$

where  $\mathbf{a}_u(t) \stackrel{\text{def}}{=} \frac{dL}{d\mathbf{u}(t)}$ . The gradients of loss w.r.t.  $\mathbf{p}(0)$ , the initial embedding of products, can be done in the same way and we omit its description for space reasons. Calculating the gradients requires a space complexity of  $\mathcal{O}(1)$  and a time complexity of  $\mathcal{O}(\frac{1}{s})$ , where  $s$  is the average step-size of underlying ODE solver which is fixed for the Euler method and RK4 and varied for DOPRI, because we use the adjoint sensitivity method.

The gradient of loss w.r.t.  $t_i$  does not involve the adjoint sensitivity method but is defined directly as follows:

$$\begin{aligned} \frac{dL}{dt_i} &= \frac{\partial L}{\partial \mathbf{u}(t_i)} \frac{d\mathbf{u}(t_i)}{dt_i} + \frac{\partial L}{\partial \mathbf{p}(t_i)} \frac{d\mathbf{p}(t_i)}{dt_i} \\ &= \mathbf{a}_u(t_i)g(\mathbf{u}(t_i)) + \mathbf{a}_p(t_i)f(\mathbf{p}(t_i)), \end{aligned} \quad (15)$$

where its complexity is  $\mathcal{O}(T)$  to train all time-points.

---

#### Algorithm 1: How to train $E_0^u$ and $E_0^p$

---

**Input:** Rating matrix  $R$

- 1 Initialize  $E_0^u$  and  $E_0^p$ ;
- 2 **while** the BPR loss  $L$  is not converged **do**
- 3     Update  $E_0^u$  with  $\frac{dL}{d\mathbf{u}(0)}$ ;
- 4     Update  $E_0^p$  with  $\frac{dL}{d\mathbf{p}(0)}$ ;
- 5     Update  $t_i$  for all  $i$ ;
- 6 **return**  $E_0^u$  and  $E_0^p$ ;

---

Table 2: Statistics of datasets

Name	#Users	#Items	#Interactions
Gowalla	29,858	40,981	1,027,370
Yelp2018	31,668	38,048	1,561,406
Amazon-Book	52,643	91,599	2,984,108

Our propose training algorithm is in Alg. 1. We alternately train each part until the BPR loss converges.

**3.3.1 On the Tractability of Training.** The Cauchy–Kowalevski theorem states that, given  $f = \frac{d\mathbf{h}(t)}{dt}$ , there exists a unique solution of  $\mathbf{h}$  if  $f$  is analytic (or locally Lipschitz continuous), i.e. the ODE problem is well-posed if  $f$  is analytic [12]. In our case, Eq. (12), which is to model  $\frac{d\mathbf{u}(t)}{dt}$  and  $\frac{d\mathbf{p}(t)}{dt}$ , uses matrix multiplications that are analytic. This implies that there will be only a unique optimal ODE for  $\mathbf{u}(t)$ , given fixed  $\mathbf{p}(t)$  and vice versa. Because of i) the uniqueness of the solution and ii) our relatively simpler definitions of  $f$  and  $g$  in comparison with other NODE applications, we believe that our training method can find a good solution.

## 4 EXPERIMENTAL EVALUATIONS

In this section, we introduce our experimental environments and results. All experiments were conducted in the following software and hardware environments: UBUNTU 18.04 LTS, PYTHON 3.6.6, NUMPY 1.18.5, SCIPY 1.5, MATPLOTLIB 3.3.1, PYTORCH 1.2.0, CUDA 10.0, and NVIDIA Driver 417.22, i9 CPU, and NVIDIA RTX TITAN.

### 4.1 Experimental Environments

**4.1.1 Datasets and Baselines.** We use the three benchmark datasets used by previous works without any modifications: Gowalla, Yelp2018, and Amazon-Book [5, 16, 34]. Their statistics are summarized in Table 2. We consider the following baselines to compare with:

- (1) MF [29] is a matrix decomposition optimized by Bayesian Personalization Rank (BPR) loss, which utilizes the user-item direct interaction only as the target value of the interaction function.
- (2) Neu-MF is a neural collaborative filtering method [18]. This method uses multiple hidden layers above the element-wise concatenation of user and item embeddings to capture their non-linear feature interactions.
- (3) CMN [11] is a state-of-the-art memory-based model. This method uses first-order connections to find similar users who interacted with the same items.

- (4) HOP-Rec [40] is a graph-based model, which uses the high-order user-item interactions by random walks to enrich the original training data.
- (5) GC-MC [30] is a graph auto-encoder framework based on differentiable message passing on the bipartite interaction graph. This method applies the GCN encoder on user-item bipartite graph and employs one convolutional layer to exploit the direct connections between users and items.
- (6) Mult-VAE is a variational autoencoder-based CF method [24]. We use a drop-out rate of  $\{0, 0.2, 0.5\}$  and  $\beta$  of  $\{0.2, 0.4, 0.6, 0.8\}$ . The layer-wise dimensionality is 600, 200, and then 600 as recommended in the paper and the authors.
- (7) GRMF is a matrix factorization method by adding the graph Laplacian regularizer [28]. We change the original loss of GRMF to the BPR loss for fair comparison. GRMF-norm is a slight variation from GRMF by adding a normalization to graph Laplacian.
- (8) NGCF [34] is a representative GCN-based CF method. It uses feature transformation and non-linear activations.
- (9) LR-GCCF [5] and LightGCN [16] are linear GCN-based CF methods. They currently show state-of-the-art accuracy.

We use the two standard evaluation metrics, Recall@20 and NDCG@20, with the all-ranking protocol, i.e., all items that do not have any interactions with a user are recommendation candidates.

**4.1.2 Hyperparameters.** Our method and the above baseline models have several common hyperparameters. In this paragraph, we introduce them.

- (1) The regularization coefficient  $\lambda$  in all methods is in  $\{1.0e-4, 1.0e-3, 1.0e-2\}$ .
- (2) The dimensionality of embedding vectors is 64 as recommended in [16], and a Normal distribution of  $\mathcal{N}(0, 0.1)$  is used to set initial embeddings.
- (3) The layer combination coefficient  $w_i = \frac{1}{1+K}$ , where  $K$  is the number of elements in the layer combination.
- (4) The number of elements  $K$  is in  $\{2, 3, 4\}$ .
- (5) The number of learnable intermediate time points  $T$  is in  $\{1, 2, 3\}$ .
- (6) We use the same early stopping criterion as that of NGCF and train with Adam and a learning rate in  $\{1.0e-5, 1.0e-4, 1.0e-3, 1.0e-2\}$ .
- (7) We consider the following ODE solvers: the explicit Euler method, RK4, Adams-Moulto, and DOPRI.

The best configuration set in each data is as follows: In Gowalla,  $\lambda = 1.0e-4$ , learning rate =  $1.0e-4$ , learning rate for time =  $1.0e-6$ ,  $K = 4$ ,  $T = 3$ ; In Yelp2018,  $\lambda = 1.0e-4$ , learning rate =  $1.0e-5$ , learning rate for time =  $1.0e-6$ ,  $K = 4$ ,  $T = 3$ ; In Amazon-Book,  $\lambda = 1.0e-4$ , learning rate =  $1.0e-4$ , learning rate =  $1.0e-6$ ,  $K = 4$ ,  $T = 3$ .

## 4.2 Experimental Results

In Table 3, we summarize the overall accuracy in terms of recall and NDCG. The non-linear GCN-based method, NGCF, shows good performance for a couple of cases in comparison with other non-GCN-based methods. After that, LightGCN shows the state-of-the-art accuracy in all cases among all baselines. It sometimes outperforms

**Table 3: Model performance comparison. LT-OCF significantly outperforms other methods in Amazon-Book.**

Dataset	Gowalla		Yelp2018		Amazon-Book	
Method	Recall	NDCG	Recall	NDCG	Recall	NDCG
MF	0.1291	0.1109	0.0433	0.0354	0.0250	0.0196
NeuMF	0.1399	0.1212	0.0451	0.0363	0.0258	0.0200
CMN	0.1405	0.1221	0.0475	0.0369	0.0267	0.0218
HOP-Rec	0.1399	0.1214	0.0517	0.0428	0.0309	0.0232
GC-MC	0.1395	0.1204	0.0462	0.0379	0.0288	0.0224
PinSage	0.1380	0.1196	0.0471	0.0393	0.0282	0.0219
Multi-VAE	0.1641	0.1335	0.0584	0.0450	0.0407	0.0315
GRMF	0.1477	0.1205	0.0571	0.0462	0.0354	0.0270
GRMF-Norm	0.1557	0.1261	0.0561	0.0454	0.0352	0.0269
NGCF	0.1570	0.1327	0.0579	0.0477	0.0344	0.0263
LR-GCCF	0.1518	0.1259	0.0574	0.0349	0.0341	0.0258
LightGCN	0.1830	0.1554	0.0649	0.0530	0.0411	0.0315
LT-OCF	<b>0.1875</b>	<b>0.1574</b>	<b>0.0671</b>	<b>0.0549</b>	<b>0.0442</b>	<b>0.0341</b>

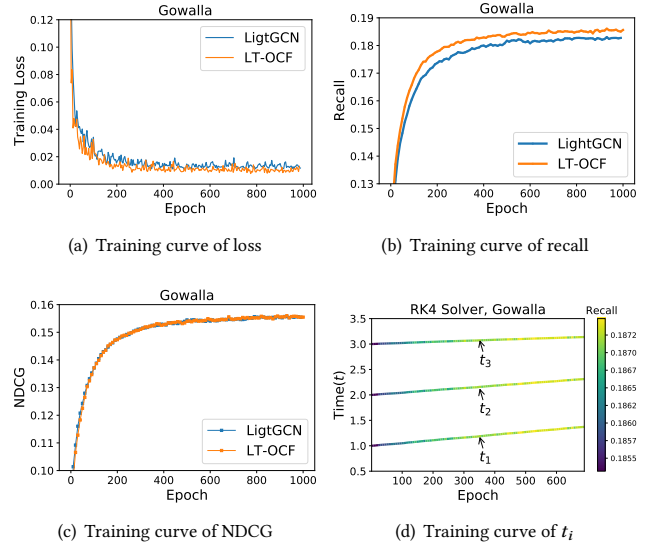


**Figure 6: Training curves in Gowalla. (a) The loss curves, (b) The training curves of Recall, (c) The training curves of NDCG, (d) The training curves of  $t_1, t_2, t_3$  when  $T = 3$ .**

other methods by large margins, e.g., a recall of 0.1830 in Gowalla by Light GCN vs. a recall of 0.1641 by Multi-VAE. In general, the three GCN-base methods, NGCF, LR-GCCF, and LightGCN, outperform other baseline methods by large margins.

However, the best accuracy is straightly marked by our method, LT-OCF, in all cases. All those best results are achieved by RK4, which implies that the linear GCN architecture of LightGCN may not be the best option (see our discussion in Section 5). In particular, our method's NDCG in Amazon-Book shows an improvement of approximately 10% over LightGCN.

In Figure 6, we compare the training curve of LightGCN and LT-OCF in Gowalla. In general, our method provides a faster training speed in terms of the number of epochs than that of LightGCN. In

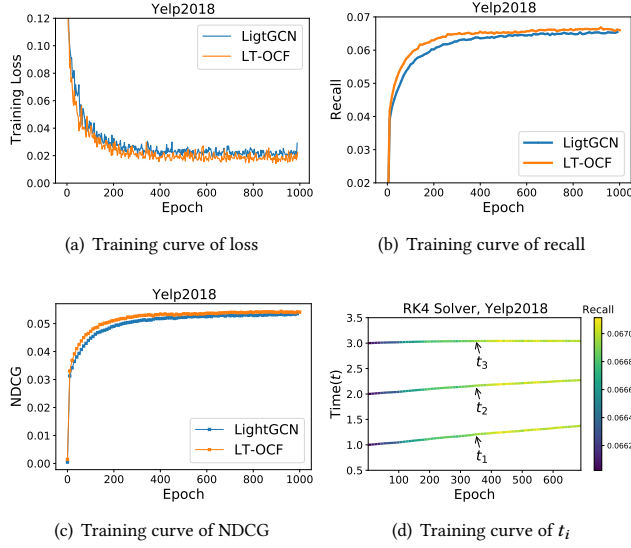


**Figure 7: Training curves in Yelp2018. (a) The loss curves, (b) The training curves of Recall, (c) The training curves of NDCG, (d) The training curves of  $t_1, t_2, t_3$  when  $T = 3$ .**

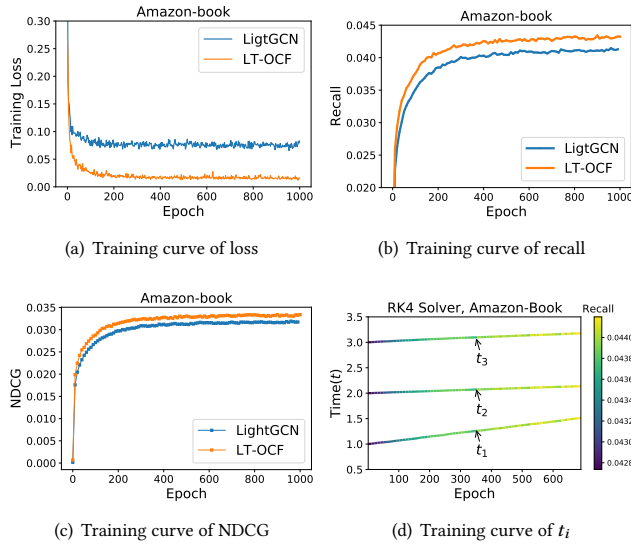


**Figure 8: Training curves in Amazon-Book. (a) The loss curves, (b) The training curves of Recall, (c) The training curves of NDCG, (d) The training curves of  $t_1, t_2, t_3$  when  $T = 3$ .**

Figure 6 (d), we show that  $t_i$  becomes larger (with a little fluctuation) as training goes on. It is because our model prefers embeddings from deep layers when constructing the layer combination.  $t_1$  is more actively trained and  $t_3$  is not trained much. According to this training pattern, we can know that it is more important to have reliable early layers for the layer combination.

In Figures 7 and 8, we show the results of the same experiment types for Yelp2018 and Amazon-Book. For Amazon-Book, LT-OCF shows remarkably smaller loss values than that of LightGCN as shown in Figure 8 (a). In Figures 7 (b,c) and 8 (b,c), our method shows faster training for recall and NDCG than LightGCN. In Figure 8 (d),  $t_1$  is trained a lot more than other cases in Figures 6 (d) and 7 (d).

### 4.3 Ablation and Sensitivity Studies

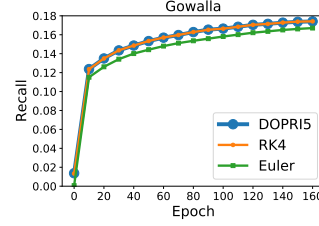


**Figure 9: Various ODE solvers**

**4.3.1 Euler vs. RK4 vs. DOPRI.** We first compare various ODE solvers. Figure 9 summarizes training curves of various ODE solvers. In general, DOPRI and RK4 are almost the same in terms of recall and NDCG while RK4 has 33% smaller computation complexity. So, we use RK4 as our default

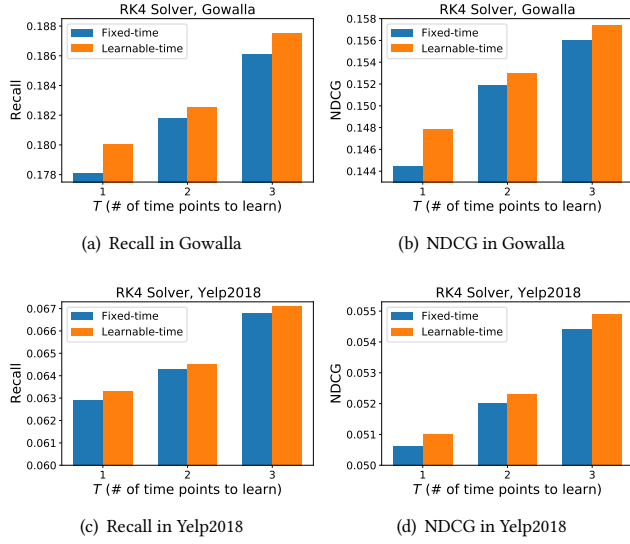
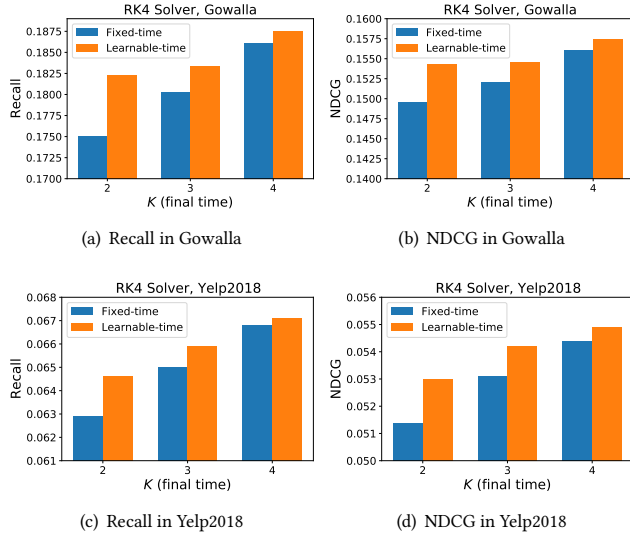
solver. As mentioned earlier, RK4 shows better accuracy than that of the Euler method in solving general ODE problems and we observe the same result. For instance, our method ( $K=4$ , learning  $t_i$ ) with the Euler method achieves a recall/NDCG of 0.1834/0.1548 vs. 0.1875/0.1574 with RK4 in Gowalla. For other datasets, we can observe similar patterns. RK4 consistently outperforms the Euler method. Adams-Moulto shows almost the same performance as that of RK4. However, it is an implicit ODE solver that requires more computation than other explicit methods, e.g., RK4.

**4.3.2 Sensitivity on  $T$ .** By varying  $T$ , we also investigate how the model accuracy changes. The detailed results are in Figure 10. One point that is worth mentioning is that the fixed-time is sometimes more vulnerable to small  $T$  than the learnable-time. In other words, the recall/NDCG gap between the fixed and the learnable-time at  $T = 1$  is larger than that in  $T = 2, 3$  for Gowalla. In general, the recall increases as we increase  $T$  but it is stabilized after  $T = 3$ . Therefore, our best setting for  $T$  is 3 in our experiments, considering computational efficiency. We can observe similar patterns in Amazon-Book as well.

**4.3.3 Sensitivity on  $K$ .** By varying  $K$ , we investigate how the model accuracy changes in Figure 11. Our best results are all made with  $K = 4$ . As decreasing  $K$ , we observe that performance also decreases. For instance, our method (RK4, learning  $t_i$ ) achieves a recall/NDCG of 0.1833/0.1545 with  $K = 3$  and a recall/NDCG of 0.1823/0.1543 with  $K = 2$  in Gowalla. Similar patterns are observed in other two datasets.

**4.3.4 Fixed vs. Learnable-time.** Without learning  $t_i$ , we fix  $t_i = \frac{K}{T+1}i$  and evaluate its accuracy. The learnable-time is one of the key concepts in our work. Without learning  $t_i$ , our method ( $K=4$ , RK4) still outperforms LightGCN in many cases but is consistently worse than our method with learning  $t_i$ . For instance, our method without learning  $t_i$  achieves a recall/NDCG of 0.1859/0.1558 vs. a recall/NDCG of 0.1875/0.1574 by our method with learning  $t_i$  in Gowalla. Similar patterns are observed in other two datasets.



Figure 10: Performance comparison by varying  $T$ Figure 11: Performance comparison by varying  $K$ 

In particular, a combination of  $K = 2$  and fixed-time shows poor performance in all cases of Figure 11. However,  $K = 2$  with learning-time surprisingly shows much improvement over it, which shows the efficacy of our proposed learnable-time concept.

#### 4.4 Runtime Analyses

We solve ODE problems in our method and as a result, need longer time to train and infer than other methods. We use Amazon-Book, the largest and the most suitable dataset for this subsection, to analyze the runtime of various algorithms. Among many baselines

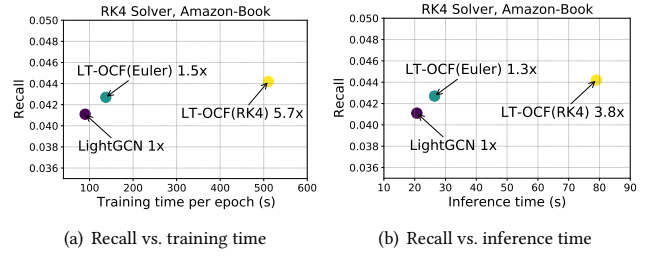


Figure 12: Training and inference time in Amazon-Book

in Table 3, we mainly compare with LightGCN since it shows state-of-the-art accuracy and has a smaller complexity than other non-linear methods. As shown in Fig. 12, LightGCN is the fastest method for both training and testing. However, our method with the Euler method provides better recall scores in 30 to 50% longer time. Even though RK4 shows the best accuracy, one can choose the Euler method to reduce the time complexity. In this regard, our proposed method is a versatile algorithm for CF, which provides a good trade-off between complexity and accuracy. Our method shows similar runtime patterns in other datasets as well.

## 5 DISCUSSIONS ON LINEAR VS. DENSE

We revisit recent debates on figuring out the best GCN architecture for CF. It was recently reported that linear layers with a layer combination work well. However, we found that dense layers with a layer combination are better. As reported in the previous section, our best accuracy was all achieved by RK4, which internally constructs connections similar to DenseNet or FractalNet as described in Table 1 [23, 25, 44]. This is well aligned with the observation in ODEs that the explicit Euler method is inferior to RK4 in solve integral problems. We conjecture that dense connections are also optimal for non-ODE-based CF methods. We leave this as an open question.

## 6 CONCLUSIONS

We tackled the problem of learnable-time ODE-based CF. Our method fundamentally differs from other methods in that we interpret the user and product embedding learning process of CF as dual co-evolving ODEs.

Owing to the continuous nature of time variable  $t$  in NODEs, we propose to train a set of time points  $\{t_1, t_2, \dots, t_T\}$ , where we extract embedding vectors to construct a layer combination architecture. Our carefully designed training method guarantees a good solution by the well-posed nature of our formulation.

With the benchmark datasets, our method, LT-OCF, consistently outperforms all state-of-the-art methods in all cases. We also showed that our method can be trained faster than other methods.

One more key contribution in this paper is that we revealed that dense connections, which are created by RK4, are the best option for our method and leave it as an open question to apply dense connections to other CF methods. We hope that this discovery will inspire forthcoming research works.

## REFERENCES

- [1] Gediminas Adomavicius and Alexander Tuzhilin. 2015. *Context-Aware Recommender Systems*. Springer US, 191–226.
- [2] James Atwood and Don Towsley. 2015. Diffusion-Convolutional Neural Networks. In *NeurIPS*. 2001–2009. arXiv:1511.02136
- [3] Joan Bruna, Wojciech Zaremba, Arthur Szlam, and Yann LeCun. 2014. Spectral networks and deep locally connected networks on graphs. In *ICLR*. 1–14. arXiv:1312.6203
- [4] Deli Chen, Yankai Lin, Wei Li, Peng Li, Jie Zhou, and Xu Sun. 2020. Measuring and Relieving the Over-Smoothing Problem for Graph Neural Networks from the Topological View. In *AAAI*.
- [5] Lei Chen, Le Wu, Richang Hong, Kun Zhang, and Meng Wang. 2020. Revisiting Graph Based Collaborative Filtering: A Linear Residual Graph Convolutional Network Approach. In *AAAI*.
- [6] R. Chen, Q. Hua, Y. Chang, B. Wang, L. Zhang, and X. Kong. 2018. A Survey of Collaborative Filtering-Based Recommender Systems: From Traditional Methods to Hybrid Methods Based on Social Networks. *IEEE Access* 6 (2018), 64301–64320.
- [7] Ricky T. Q. Chen, Yulia Rubanova, Jesse Bettencourt, and David K Duvenaud. 2018. Neural Ordinary Differential Equations. In *NeurIPS*.
- [8] Michaël Defferrard, Xavier Bresson, and Pierre Vandergheynst. 2016. Convolutional Neural Networks on Graphs with Fast Localized Spectral Filtering. In *NeurIPS*. 3844–3852. arXiv:1606.09375
- [9] J.R. Dormand and P.J. Prince. 1980. A family of embedded Runge-Kutta formulae. *J. Comput. Appl. Math.* 6, 1 (1980), 19 – 26.
- [10] Emilien Dupont, Arnaud Doucet, and Yee Whye Teh. 2019. Augmented Neural ODEs. In *NeurIPS*.
- [11] Travis Ebesu, Bin Shen, and Yi Fang. 2018. Collaborative Memory Network for Recommendation Systems. In *SIGIR*. ACM, 515–524.
- [12] GERALD B. FOLLAND. 1995. *Introduction to Partial Differential Equations: Second Edition*. Vol. 102. Princeton University Press.
- [13] Hongyang Gao, Zhengyang Wang, and Shuiwang Ji. 2018. Large-Scale Learnable Graph Convolutional Networks. In *SIGKDD*. 1416–1424. <https://doi.org/10.1145/3219819.3219947> arXiv:1808.03965
- [14] Justin Gilmer, Samuel S. Schoenholz, Patrick F. Riley, Oriol Vinyals, and George E. Dahl. 2017. Neural Message Passing for Quantum Chemistry. *ICML* 3 (apr 2017), 2053–2070. arXiv:1704.01212
- [15] William L. Hamilton, Rex Ying, and Jure Leskovec. 2017. Inductive Representation Learning on Large Graphs. In *NeurIPS*, Vol. 2017-Decem. arXiv:1706.02216
- [16] Xiangnan He, Kuan Deng, Xiang Wang, Yan Li, YongDong Zhang, and Meng Wang. 2020. LightGCN: Simplifying and Powering Graph Convolution Network for Recommendation. In *SIGIR*.
- [17] X. He, Z. He, J. Song, Z. Liu, Y. Jiang, and T. Chua. 2018. NAIS: Neural Attentive Item Similarity Model for Recommendation. *IEEE Transactions on Knowledge and Data Engineering* 30, 12 (2018), 2354–2366.
- [18] Xiangnan He, Lizi Liao, Hanwang Zhang, Liqiang Nie, Xia Hu, and Tat-seng Chua. 2017. Neural Collaborative Filtering. In *WWW*. 173–182.
- [19] Thomas N. Kipf and Max Welling. 2017. Semi-Supervised Classification with Graph Convolutional Networks. In *ICLR*.
- [20] Yehuda Koren. 2008. Factorization Meets the Neighborhood: A Multifaceted Collaborative Filtering Model. In *KDD*.
- [21] Yehuda Koren. 2010. Factor in the neighbors. *ACM Transactions on Knowledge Discovery from Data* 4 (2010), 1–24.
- [22] Y. Koren, R. Bell, and C. Volinsky. 2009. Matrix Factorization Techniques for Recommender Systems. *Computer* 42, 8 (2009), 30–37.
- [23] Gustav Larsson, M. Maire, and Gregory Shakhnarovich. 2017. FractalNet: Ultra-Deep Neural Networks without Residuals. In *ICLR*.
- [24] Dawen Liang, Rahul G. Krishnan, Matthew D. Hoffman, and Tony Jebara. 2018. Variational Autoencoders for Collaborative Filtering. In *TheWebConf (former WWW)*.
- [25] Yiping Lu, Aoxiao Zhong, Quanzheng Li, and Bin Dong. 2018. Beyond Finite Layer Neural Networks: Bridging Deep Architectures and Numerical Differential Equations. In *ICML*.
- [26] Stefano Massaroli, Michael Poli, Jinkyoo Park, Atsushi Yamashita, and Hajime Asama. 2020. Dissecting Neural ODEs. arXiv:2002.08071 [cs.LG]
- [27] Hans Pinckaers and Geert Litjens. 2019. Neural Ordinary Differential Equations for Semantic Segmentation of Individual Colon Glands. arXiv:1910.10470 (2019).
- [28] Nikhil Rao, Hsiang-Fu Yu, Pradeep K Ravikumar, and Inderjit S Dhillon. 2015. Collaborative Filtering with Graph Information: Consistency and Scalable Methods. In *NeurIPS*.
- [29] Steffen Rendle, Christoph Freudenthaler, Zeno Gantner, and Lars Schmidt-Thieme. 2009. BPR: Bayesian Personalized Ranking from Implicit Feedback. In *UAI*.
- [30] Rianne van den Berg, Thomas N. Kipf, and Max Welling. 2017. Graph Convolutional Matrix Completion. *CoRR* abs/1706.02263 (2017). arXiv:1706.02263
- [31] Petar Veličković, Guillem Cucurull, Arantxa Casanova, Adriana Romero, Pietro Liò, and Yoshua Bengio. 2017. Graph Attention Networks. In *ICLR 2018*. 1–12. arXiv:1710.10903
- [32] Hao Wang, Naiyan Wang, and Dit-Yan Yeung. 2014. Collaborative Deep Learning for Recommender Systems. In *KDD*, Vol. 2015-Augus. 1235–1244.
- [33] Hongwei Wang, Miao Zhao, Xing Xie, Wenjie Li, and Minyi Guo. 2019. Knowledge Graph Convolutional Networks for Recommender Systems. In *TheWebConference*.
- [34] Xiang Wang, Xiangnan He, Meng Wang, Fuli Feng, and Tat-Seng Chua. 2019. Neural Graph Collaborative Filtering. In *SIGIR*.
- [35] Yinwei Wei, Xiang Wang, Liqiang Nie, Xiangnan He, Richang Hong, and Tat-Seng Chua. 2019. MMGCN: Multi-modal Graph Convolution Network for Personalized Recommendation of Micro-video. In *MM*.
- [36] Felix Wu, Tianyi Zhang, Amauri Holanda de Souza, Christopher Fifty, Tao Yu, and Kilian Q. Weinberger. 2019. Simplifying Graph Convolutional Networks. In *ICML*, Vol. 2019-June. 11884–11894. arXiv:1902.07153
- [37] Yao Wu, Christopher DuBois, Alice X. Zheng, and Martin Ester. 2016. Collaborative Denoising Auto-Encoders for Top-N Recommender Systems. In *Proceedings of the Ninth ACM International Conference on Web Search and Data Mining*. ACM, New York, NY, USA, 153–162.
- [38] Bingbing Xu, HuaWei Shen, Qi Cao, Yunqi Qiu, and Xueqi Cheng. 2019. Graph Wavelet Neural Network. In *ICLR*. 1–13. arXiv:1904.07785
- [39] Hanshu Yan, Jiawei Du, Vincent Y. F. Tan, and Jiashi Feng. 2020. On Robustness of Neural Ordinary Differential Equations. arXiv:1910.05513
- [40] Jheng-Hong Yang, Chih-Ming Chen, Chuan-Ju Wang, and Ming-Feng Tsai. 2018. HOP-rec: high-order proximity for implicit recommendation. In *Proceedings of the 12th ACM Conference on Recommender Systems*. 140–144.
- [41] Zhe Yang, Bing Wu, Kan Zheng, Xianbin Wang, and Lei Lei. 2016. A Survey of Collaborative Filtering-Based Recommender Systems for Mobile Internet Applications. *IEEE Access* 4 (2016), 3273–3287.
- [42] Rex Ying, Ruining He, Kaifeng Chen, Pong Eksombatchai, William L. Hamilton, and Jure Leskovec. 2018. Graph Convolutional Neural Networks for Web-Scale Recommender Systems. In *KDD*.
- [43] Shuai Zhang, Lina Yao, Aixin Sun, and Yi Tay. 2019. Deep Learning Based Recommender System: A Survey and New Perspectives. *ACM Comput. Surv.* 52, 1 (2019).
- [44] Mai Zhu, Bo Chang, and Chong Fu. 2019. Convolutional Neural Networks combined with Runge-Kutta Methods. arXiv:1802.08831

## A BEST HYPERPARAMETERS

We list the best hyperparameter configurations as follows:

- (1) In Gowalla,  $\lambda = 1.0e-4$ , learning rate =  $1.0e-4$ , learning rate for time =  $1.0e-6$ ,  $K = 4$ ,  $T = 3$ ;
- (2) In Yelp2018,  $\lambda = 1.0e-4$ , learning rate =  $1.0e-5$ , learning rate for time =  $1.0e-6$ ,  $K = 4$ ,  $T = 3$ ;
- (3) In Amazon-Book,  $\lambda = 1.0e-4$ , learning rate =  $1.0e-4$ , learning rate =  $1.0e-6$ ,  $K = 4$ ,  $T = 3$ .

## B ADDITIONAL EXPERIMENTAL RESULTS

In the main papers, we have use Recall@20 and NDCG@20. We report other cases in this section. We compare only our method with various settings. RK4 and Adams-Moulto consistently show the best accuracy.

Table 7 shows the training time per epoch and the inference time for the entire testing data by various ODE solvers.

**Table 4: Model performance of Recall@N, Precision@N and NDCG@N on Gowalla dataset.**

	Solver	Explicit Euler	RK4	Adams-Moulto
N=10	Recall	0.1295	0.1323	0.1323
	NDCG	0.1389	0.1641	0.1641
	Precision	0.0778	0.0792	0.0792
N=20	Recall	0.1834	0.1875	0.1875
	NDCG	0.1548	0.1574	0.1574
	Precision	0.0562	0.0571	0.0571
N=30	Recall	0.2239	0.2280	0.2280
	NDCG	0.1679	0.1706	0.1706
	Precision	0.0461	0.0469	0.0469
N=40	Recall	0.2562	0.2610	0.2610
	NDCG	0.1781	0.1812	0.1812
	Precision	0.0398	0.0406	0.0406
N=50	Recall	0.2849	0.2899	0.2899
	NDCG	0.1868	0.1898	0.1898
	Precision	0.0356	0.0361	0.0361

**Table 5: Model performance of Recall@N, Precision@N and NDCG@N on Yelp2018 dataset.**

	Solver	Explicit Euler	RK4	Adams-Moulto
N=10	Recall	0.0385	0.0393	0.0393
	NDCG	0.0441	0.0447	0.0447
	Precision	0.0344	0.0347	0.0347
N=20	Recall	0.0661	0.0671	0.0671
	NDCG	0.0541	0.0549	0.0549
	Precision	0.0296	0.0299	0.0299
N=30	Recall	0.0888	0.0901	0.0901
	NDCG	0.0629	0.0637	0.0637
	Precision	0.0266	0.0299	0.0299
N=40	Recall	0.1084	0.1100	0.1100
	NDCG	0.0701	0.0711	0.0711
	Precision	0.0245	0.0248	0.0248
N=50	Recall	0.1263	0.1282	0.1282
	NDCG	0.0764	0.0778	0.0778
	Precision	0.0229	0.0233	0.0233

**Table 6: Model performance of Recall@N, Precision@N and NDCG@N on Amazon-Book dataset.**

	Solver	Explicit Euler	RK4	Adams-Moulto
N=10	Recall	0.2440	0.2553	0.2553
	NDCG	0.0254	0.0265	0.0265
	Precision	0.0198	0.0201	0.0201
N=20	Recall	0.0427	0.0442	0.0442
	NDCG	0.0327	0.0341	0.0341
	Precision	0.0176	0.0181	0.0181
N=30	Recall	0.0578	0.0594	0.0594
	NDCG	0.0386	0.0399	0.0399
	Precision	0.0160	0.0165	0.0165
N=40	Recall	0.0706	0.0729	0.0729
	NDCG	0.0433	0.0449	0.0449
	Precision	0.0149	0.0153	0.0153
N=50	Recall	0.0827	0.0853	0.0853
	NDCG	0.0476	0.0492	0.0492
	Precision	0.0140	0.0145	0.0145

**Table 7: Training time per epoch and inference time in each dataset.**

Dataset	Time(s)	Explicit Euler	RK4	Adams-Moulto
Gowalla	Training	17.05	59.84	59.40
	Inference	7.40	17.35	17.61
Yelp2018	Training	34.49	125.67	127.60
	Inference	8.99	20.71	23.38
Amazon-Book	Training	137.42	510.76	512.23
	Inference	24.46	79.0	80.19

## C LINEAR GCNS AND NEWTON’S LAW OF COOLING

The linear graph convolutional layer of LightGCN in Eq. (5) can be seen as a numerical discretization of the corresponding continuous graph heat equation:

$$\frac{dH_t}{dt} = -\Delta H_t = -LH_t, \quad (16)$$

where the finite difference interval of time  $dt$  is 1, the final time  $K$  is  $T + 1$ ,  $H_t$  is a column vector that includes the temperature values of nodes in a graph, and

$$L = D^{-1/2}(D - \tilde{A})D^{-1/2} = I - \tilde{A} \quad (17)$$

is the symmetrically normalized graph Laplacian operator.

When applying the Euler discretization to Eq. (16) with an interval step size  $dt = \frac{K}{T+1}$ , we have

$$\begin{aligned} H_{t+dt} &= H_t - dtLH_t \\ &= H_t - dt(I - \tilde{A})H_t \\ &= [(1 - dt)I + dt\tilde{A}]H_t. \end{aligned} \quad (18)$$

We will get the following final  $H_K$ , if we keep evolving the ODE until the terminal time  $K = dt(T + 1)$ .

$$H_K = [\tilde{A}^{dt}]^{T+1}H. \quad (19)$$

We regard that LightGCN corresponds to the Euler discretization with a large step size  $dt = 1$ . This step size reduces the diffusion matrix to the Linear GCN diffusion matrix  $\tilde{A}$ .

$$\tilde{A}^{(dt)}|_{dt=1} = (1 - 1)I + \tilde{A} = \tilde{A} \quad (20)$$

and the final  $H$  becomes equivalent:

$$H_K|_{dt=1} = H_{T+1} = H^{(T+1)} = \tilde{A}^{T+1}H. \quad (21)$$

Then we can consider  $H$  as a product or user embedding, because we interpret each element of  $E_i^u$  and  $E_i^p$  as a temperature value. Therefore, we take the LightGCN model from the continuous thermal diffusive processes.